

# Circuit QED: single-step realization of a multiqubit controlled phase gate with one microwave photonic qubit simultaneously controlling $n - 1$ microwave photonic qubits

Biaoliang Ye<sup>1</sup>, Zhen-Fei Zheng<sup>2</sup>, Yu Zhang<sup>3</sup>, and Chui-Ping Yang<sup>1,4\*</sup>

<sup>1</sup>*Quantum Information Research Center,*

*Shangrao Normal University, Shangrao 334001, China*

<sup>2</sup>*CAS Key Laboratory of Quantum Information,*

*University of Science and Technology of China, Hefei 230026, China*

<sup>3</sup>*School of Physics, Nanjing University, Nanjing 210093, China and*

<sup>4</sup>*Department of Physics, Hangzhou Normal University, Hangzhou 310036, China*

## Abstract

We present a novel method to realize a multi-target-qubit controlled phase gate with one microwave photonic qubit simultaneously controlling  $n - 1$  target microwave photonic qubits. This gate is implemented with  $n$  microwave cavities coupled to a superconducting flux qutrit. Each cavity hosts a microwave photonic qubit, whose two logic states are represented by the vacuum state and the single photon state of a single cavity mode, respectively. During the gate operation, the qutrit remains in the ground state and thus decoherence from the qutrit is greatly suppressed. This proposal requires only a single-step operation and thus the gate implementation is quite simple. The gate operation time is independent of the number of the qubits. In addition, this proposal does not need applying classical pulse or any measurement. Numerical simulations demonstrate that high-fidelity realization of a controlled phase gate with one microwave photonic qubit simultaneously controlling two target microwave photonic qubits is feasible with current circuit QED technology. The proposal is quite general and can be applied to implement the proposed gate in a wide range of physical systems, such as multiple microwave or optical cavities coupled to a natural or artificial  $\Lambda$ -type three-level atom.

PACS numbers:

---

\*Electronic address: yangcp@hznu.edu.cn

## I. INTRODUCTION

Multiple qubit gates play important roles and are a crucial element in quantum information processing (QIP). A multiqubit gate can in principle be decomposed into a series of two-qubit and single-qubit gates, and thus can be constructed by using these basic gates. However, it is commonly recognized that building a multiqubit gate is difficult via the conventional gate-decomposition protocol. This is because the number of basic gates, required for constructing a multiqubit gate, increases drastically as the number of qubits increases. As a result, the gate operation time would be quite long and thus the gate fidelity would be significantly decreased by decoherence. Hence, it is worthwhile to seek efficient approaches to realize multiqubit quantum gates. Many efficient schemes have been presented for the direct realization of a multiqubit controlled-phase or controlled-NOT gate, with multiple-control qubits acting on one target qubit [1–14]. This type of multiqubit gate is of significance in QIP, such as quantum algorithms and error corrections.

In this work, we focus on another type of multiqubit gate, i.e., a multi-target-qubit controlled phase gate with one qubit simultaneously controlling multiple target qubits. This multi-target-qubit controlled phase gate is described by

$$\begin{aligned} |0_1\rangle |i_2\rangle |i_3\rangle \dots |i_n\rangle &\rightarrow |0_1\rangle |i_2\rangle |i_3\rangle \dots |i_n\rangle, \\ |1_1\rangle |i_2\rangle |i_3\rangle \dots |i_n\rangle &\rightarrow |1_1\rangle (-1)^{i_2} (-1)^{i_3} \dots (-1)^{i_n} |i_2\rangle |i_3\rangle \dots |i_n\rangle, \end{aligned} \quad (1)$$

where  $i_2, i_3, \dots, i_n \in \{0, 1\}$ ; subscript 1 represents the control qubit while subscripts 2, 3,  $\dots$ , and  $n$  represent target qubits. From Eq. (1), it can be seen that when the control qubit 1 is in  $|1\rangle$ , a phase flip (from sign  $+$  to  $-$ ) happens to the state  $|1\rangle$  of each of target qubits 2, 3,  $\dots$ , and  $n$ ; however nothing happens to the states of each of target qubits 2, 3,  $\dots$ , and  $n$  when the control qubit 1 is in the state  $|0\rangle$ .

This multiqubit gate (1) is useful in QIP, such as entanglement preparation [15], error correction [16], quantum algorithms [17], and quantum cloning [18]. How to efficiently implement this multiqubit gate becomes necessary and important. Over the past years, based on cavity QED or circuit QED, many efficient methods have been proposed for the direct implementation of this multiqubit phase gate, by using natural atoms or artificial atoms (e.g., superconducting qubits, quantum dots, or nitrogen-vacancy center ensembles) [19–23].

Circuit QED is analogue of cavity QED, which consists of superconducting qubits and microwave resonators or cavities. It has developed fast recently and is considered as one of the most promising candidates for QIP [23–29]. Owing to the microfabrication technology scalability, individual qubit addressability, and ever-increasing qubit coherence time [30–38], superconducting qubits are of great importance in QIP. The strong and ultrastrong couplings between a superconducting qubit and a microwave cavity have been experimentally demonstrated [39,40]. For a review on the ultrastrong coupling, refer to [41]. On the other hand, a (loaded) quality factor  $Q \sim 10^6$  has been experimentally reported for a one-dimensional coplanar waveguide microwave resonator [42,43], and a (loaded) quality factor  $Q \sim 3.5 \times 10^7$  has also been experimentally reported for a three-dimensional microwave cavity [44]. A microwave resonator or cavity with the experimentally-reported high quality factor here can act as a good quantum data bus [45–47] and be used as a good quantum memory [48,49], because it contains microwave photons whose lifetimes are much longer than that of a superconducting qubit [50]. These good features make microwave resonators or cavities as a powerful platform for quantum computation and microwave photons as one of promising qubits for QIP. Recently, quantum state engineering and QIP with microwave fields or photons have become considerably interesting [51-72].

Motivated by the above, we will propose a method to realize the multi-target-qubit controlled phase gate (1) with microwave photonic qubits, by using  $n$  microwave cavities coupled to a superconducting flux qutrit (a  $\Lambda$ -type three-level artificial atom) (Fig. 1). Note that to simplify the presentation, we will use “MP qubit” to denote “microwave photonic qubit” and “MP qubits” to define “microwave photonic qubits”. This work is based on circuit QED. As shown below, this proposal has the following advantages: (i) During the gate operation, the qutrit stays in the ground state and thus decoherence from the qutrit is greatly suppressed; (ii) Because of only using one-step operation, the gate implementation is quite simple; (iii) Neither classical pulse nor measurement is required; (iv) The gate operation time is independent of the number of the qubits; and (v) This proposal is quite general and can be extended to a wide range of physical systems to realize the proposed gate, such as multiple microwave or optical cavities coupled to a natural or artificial  $\Lambda$ -type three-level atom. To the best of our knowledge, this work is the first to show the one-step implementation of a multi-target-qubit controlled phase gate with MP qubits, based on cavity- or circuit-QED and without any measurement.

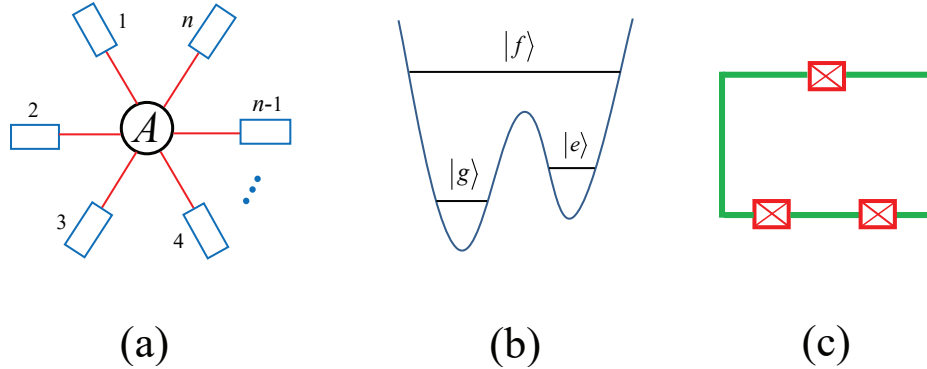


FIG. 1: (a) Diagram of  $n$  cavities ( $1, 2, \dots, n$ ) coupled to a superconducting flux qutrit  $A$ . A square represents a cavity, which can be a one-dimensional or three-dimensional cavity. The qutrit is capacitively or inductively coupled to each cavity. (b) Level configuration of the flux qutrit, for which the transition between the two lowest levels can be made weak by increasing the barrier between two potential wells. (c) Diagram of a flux qutrit, which consists of three Josephson junctions and a superconducting loop.

This paper is organized as follows. In Sec. II, we explicitly show how to realize a controlled-phase gate with one MP qubit simultaneously controlling  $n - 1$  target MP qubits. In Sec. III, we discuss the experimental feasibility for implementing a three-qubit controlled phase gate, by considering a setup of three one-dimensional transmission line resonators coupled to a superconducting flux qutrit. We end up with a conclusion in Sec. IV.

## II. MULTI-TARGET-QUBIT CONTROLLED PHASE GATE

Consider  $n$  microwave cavities ( $1, 2, \dots, n$ ) coupled to a superconducting flux qutrit [Fig. 1(a)]. The three levels of the qutrit are denoted as  $|g\rangle$ ,  $|e\rangle$  and  $|f\rangle$ , as shown in Fig. 1(b). In general, there exists the transition between the two lowest levels  $|g\rangle$  and  $|e\rangle$ , which, however, can be made to be weak by increasing the barrier between the two potential wells. Suppose that cavity 1 is dispersively coupled to the  $|g\rangle \leftrightarrow |f\rangle$  transition of the qutrit with coupling constant  $g_1$  and detuning  $\delta_1$  but highly detuned (decoupled) from the  $|e\rangle \leftrightarrow |f\rangle$  transition of the qutrit. In addition, assume that cavity  $l$  ( $l = 2, 3, \dots, n$ ) is dispersively coupled to the  $|e\rangle \leftrightarrow |f\rangle$  transition of the qutrit with coupling constant  $g_l$  and detuning  $\delta_l$  but highly detuned (decoupled) from the  $|g\rangle \leftrightarrow |f\rangle$  transition of the qutrit (Fig. 2). Note that

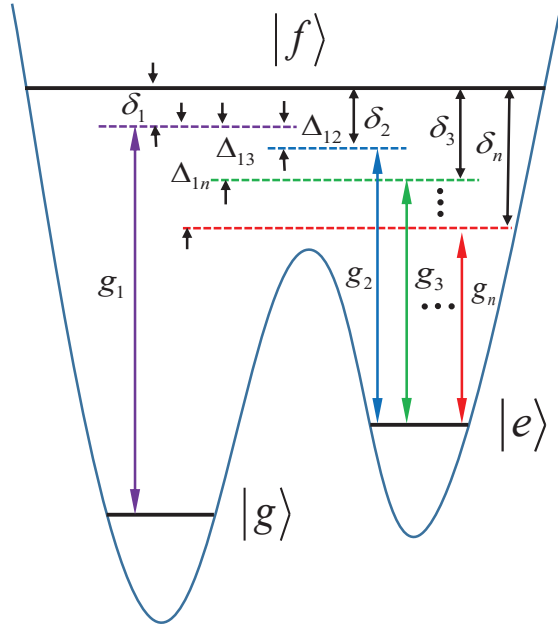


FIG. 2: Cavity 1 is dispersively coupled to the  $|g\rangle \leftrightarrow |f\rangle$  transition of the qutrit with coupling strength  $g_1$  and detuning  $\delta_1$ , while cavity  $l$  ( $l = 2, 3, \dots, n$ ) is dispersively coupled to the  $|e\rangle \leftrightarrow |f\rangle$  transition of the qutrit with coupling strength  $g_l$  and detuning  $\delta_l$ . The purple vertical line represents the frequency  $\omega_{c_1}$  of cavity 1, while the blue, green, ..., and red vertical lines represent the frequency  $\omega_{c_2}$  of cavity 2, the frequency  $\omega_{c_3}$  of cavity 3, ..., and the frequency  $\omega_{c_n}$  of cavity  $n$ , respectively.

these conditions can be satisfied by prior adjustment of the qutrit's level spacings or/and the cavity frequency. For a superconducting qutrit, the level spacings can be rapidly (within 1-3 ns) tuned by varying external control parameters (e.g., magnetic flux applied to the loop of a superconducting phase, transmon [73], Xmon [33], or flux qubit/qutrit [74]). In addition, the frequency of a microwave cavity or resonator can be rapidly adjusted with a few nanoseconds [75,76].

Under the above assumptions and by considering the ideal cavities, the Hamiltonian of the whole system, in the interaction picture and after making the rotating-wave approximation (RWA), can be written as (in units of  $\hbar = 1$ )

$$H_I = g_1(e^{-i\delta_1 t} \hat{a}_1^+ \sigma_{fg}^- + h.c.) + \sum_{l=2}^n g_l(e^{-i\delta_l t} \hat{a}_l^+ \sigma_{fe}^- + h.c.), \quad (2)$$

where  $\sigma_{fg}^- = |g\rangle\langle f|$ ,  $\sigma_{fe}^- = |e\rangle\langle f|$ ,  $\delta_1 = \omega_{fg} - \omega_{c_1} > 0$ , and  $\delta_l = \omega_{fe} - \omega_{c_l} > 0$ . The detunings  $\delta_1$  and  $\delta_l$  have a relationship  $\delta_l = \delta_1 + \Delta_{1l}$ , with  $\Delta_{1l} = \omega_{c_1} - \omega_{c_l} - \omega_{eg} > 0$  (Fig. 2). Here,

$\hat{a}_1$  ( $\hat{a}_l$ ) is the photon annihilation operator of cavity 1 ( $l$ ),  $\omega_{c_l}$  is the frequency of cavity  $l$  ( $l = 2, 3, \dots, n$ ); while  $\omega_{fg}$ ,  $\omega_{fe}$ , and  $\omega_{eg}$  are the  $|f\rangle \leftrightarrow |g\rangle$ ,  $|f\rangle \leftrightarrow |e\rangle$ , and  $|e\rangle \leftrightarrow |g\rangle$  transition frequencies of the qutrit, respectively.

Under the large-detuning conditions  $\delta_1 \gg g_1$  and  $\delta_l \gg g_l$ , the Hamiltonian (2) becomes [77]

$$\begin{aligned}
H_e = & -\lambda_1(\hat{a}_1^+\hat{a}_1|g\rangle\langle g| - \hat{a}_1\hat{a}_1^+|f\rangle\langle f|) \\
& - \sum_{l=2}^n \lambda_l(\hat{a}_l^+\hat{a}_l|e\rangle\langle e| - \hat{a}_l\hat{a}_l^+|f\rangle\langle f|) \\
& - \sum_{l=2}^n \lambda_{1l}(e^{i\Delta_{1l}t}\hat{a}_1^+\hat{a}_l\sigma_{eg}^- + h.c.) \\
& + \sum_{k \neq l; k, l=2}^n \lambda_{kl}(e^{i\Delta_{kl}t}\hat{a}_k^+\hat{a}_l + h.c.) (|f\rangle\langle f| - |e\rangle\langle e|), \tag{3}
\end{aligned}$$

where  $\lambda_1 = g_1^2/\delta_1$ ,  $\lambda_l = g_l^2/\delta_l$ ,  $\lambda_{1l} = (g_1g_l/2)(1/\delta_1 + 1/\delta_l)$ ,  $\lambda_{kl} = (g_kg_l/2)(1/\delta_k + 1/\delta_l)$ ,  $\Delta_{1l} = \delta_l - \delta_1 = \omega_{c_1} - \omega_{c_l} - \omega_{eg}$ ,  $\Delta_{kl} = \delta_l - \delta_k = \omega_{c_k} - \omega_{c_l}$ , and  $\sigma_{eg}^- = |g\rangle\langle e|$ . In Eq. (3), the terms in the first two lines describe the photon number dependent stark shifts of the energy levels  $|g\rangle$ ,  $|e\rangle$  and  $|f\rangle$ ; the terms in the third line describe the  $|e\rangle \leftrightarrow |g\rangle$  coupling caused due to the cooperation of cavities 1 and  $l$ ; while the terms in the last line describe the coupling between cavities  $k$  and  $l$ . For  $\Delta_{1l} \gg \{\lambda_1, \lambda_l, \lambda_{1l}, \lambda_{kl}\}$ , the effective Hamiltonian  $H_e$  changes to [77]

$$\begin{aligned}
H_e = & -\lambda_1(\hat{a}_1^+\hat{a}_1|g\rangle\langle g| - \hat{a}_1\hat{a}_1^+|f\rangle\langle f|) \\
& - \sum_{l=2}^n \lambda_l(\hat{a}_l^+\hat{a}_l|e\rangle\langle e| - \hat{a}_l\hat{a}_l^+|f\rangle\langle f|) \\
& - \sum_{l=2}^n \chi_{1l}(\hat{a}_1^+\hat{a}_1\hat{a}_l\hat{a}_l^+|g\rangle\langle g| - \hat{a}_1\hat{a}_1^+\hat{a}_l^+\hat{a}_l|e\rangle\langle e|) \\
& + \sum_{k \neq l; k, l=2}^n \lambda_{kl}(e^{i\Delta_{kl}t}\hat{a}_k^+\hat{a}_l + h.c.) (|f\rangle\langle f| - |e\rangle\langle e|), \tag{4}
\end{aligned}$$

where  $\chi_{1l} = \lambda_{1l}^2/\Delta_{1l}$ . From this equation, one can see that each term is associated with the level  $|g\rangle$ ,  $|e\rangle$ , or  $|f\rangle$ . When the levels  $|e\rangle$  and  $|f\rangle$  are initially not occupied, they will remain unpopulated because neither  $|g\rangle \rightarrow |e\rangle$  nor  $|g\rangle \rightarrow |f\rangle$  is induced under the Hamiltonian (4). Hence, the Hamiltonian (4) reduces to

$$H_e = -\lambda_1\hat{a}_1^+\hat{a}_1|g\rangle\langle g| - \sum_{l=2}^n \chi_{1l}\hat{a}_1^+\hat{a}_1\hat{a}_l\hat{a}_l^+|g\rangle\langle g|. \tag{5}$$

Note that  $[a_l, a_l^+] = 1$ , i.e.,  $\hat{a}_l \hat{a}_l^+ = 1 + \hat{a}_l^+ \hat{a}_l$ . Thus, the Hamiltonian (5) can be rewritten as

$$H_e = -\lambda_1 \hat{n}_1 |g\rangle\langle g| - \sum_{l=2}^n \chi_{1l} \hat{n}_1 |g\rangle\langle g| - \sum_{l=2}^n \chi_{1l} \hat{n}_1 \hat{n}_l |g\rangle\langle g|, \quad (6)$$

where  $\hat{n}_1 = \hat{a}_1^+ \hat{a}_1$  and  $\hat{n}_l = \hat{a}_l^+ \hat{a}_l$  are the photon number operators for cavities 1 and  $l$ , respectively.

Assume that the qutrit is initially in the ground state  $|g\rangle$ . It will remain in this state because the Hamiltonian (6) cannot induce any transition for the qutrit. Therefore, the Hamiltonian  $H_e$  reduces to

$$\tilde{H}_e = -\eta \hat{n}_1 - \chi \sum_{l=2}^n \hat{n}_1 \hat{n}_l, \quad (7)$$

where  $\eta = \lambda_1 + (n-1)\chi$ . Here, we have set  $\chi_{1l} = \chi$  ( $l = 2, 3, \dots, n$ ). Note that the  $\tilde{H}_e$  is the effective Hamiltonian governing the dynamics of the  $n$  cavities (1, 2, ...,  $n$ ).

The unitary operator  $U = e^{-i\tilde{H}_e t}$  can be written as

$$U = U_1 [\otimes_{l=2}^n U_{1l}], \quad (8)$$

with

$$U_1 = \exp(i\eta \hat{n}_1 t), \quad (9)$$

$$U_{1l} = \exp(i\chi \hat{n}_1 \hat{n}_l t), \quad (10)$$

where  $\otimes_{l=2}^n U_{1l} = U_{12} U_{13} \dots U_{1n}$ . Here,  $U_1$  is a unitary operator on cavity 1, while  $U_{1l}$  is a unitary operator on cavities 1 and  $l$ .

Let us now consider  $n$  MP qubits 1, 2, ..., and  $n$ , which are hosted by cavities 1, 2, ..., and  $n$ , respectively. The two logical states of MP qubit  $l'$  are represented by the vacuum state  $|0\rangle$  and the single-photon state  $|1\rangle$  of cavity  $l'$  ( $l' = 1, 2, \dots, n$ ). Based on Eq. (10), one can easily see that for  $\chi t = \pi$ , the unitary operation  $U_{1l}$  leads to the following state transformation

$$\begin{aligned} U_{1l}|0_1 0_l\rangle &= |0_1 0_l\rangle, \\ U_{1l}|0_1 1_l\rangle &= |0_1 1_l\rangle, \\ U_{1l}|1_1 0_l\rangle &= |1_1 0_l\rangle, \\ U_{1l}|1_1 1_l\rangle &= -|1_1 1_l\rangle, \end{aligned} \quad (11)$$

which implies that the operator  $U_{1l}$  implements a universal controlled-phase gate on two qubits 1 and  $l$ . Eq. (11) can be expressed as

$$\begin{aligned} U_{1l}|0_1 i_l\rangle|g\rangle &= |0_1 i_l\rangle|g\rangle \\ U_{1l}|1_1 i_l\rangle|g\rangle &= (-1)^{i_l} |1_1 i_l\rangle|g\rangle, \end{aligned} \quad (12)$$

where  $i_l \in \{0, 1\}$ .

Based on Eq. (12), one can easily obtain the following state transformation

$$\begin{aligned} \otimes_{l=2}^n U_{1l} |0_1\rangle |i_2\rangle |i_3\rangle \dots |i_n\rangle &= |0_1\rangle |i_2\rangle |i_3\rangle \dots |i_n\rangle, \\ \otimes_{l=2}^n U_{1l} |1_1\rangle |i_2\rangle |i_3\rangle \dots |i_n\rangle &= |1_1\rangle (-1)^{i_2} (-1)^{i_3} \dots (-1)^{i_n} |i_2\rangle |i_3\rangle \dots |i_n\rangle. \end{aligned} \quad (13)$$

According to (9), one can see that for  $\eta t = 2m\pi$  ( $m$  is a positive integer), the unitary operator  $U_1$  leads to

$$U_1|0_1\rangle = |0_1\rangle, \quad U_1|1_1\rangle = |1_1\rangle. \quad (14)$$

Combining Eq. (13) and Eq. (14), we have

$$\begin{aligned} U_1 [\otimes_{l=2}^n U_{1l}] |0_1\rangle |i_2\rangle |i_3\rangle \dots |i_n\rangle &= |0_1\rangle |i_2\rangle |i_3\rangle \dots |i_n\rangle, \\ U_1 [\otimes_{l=2}^n U_{1l}] |1_1\rangle |i_2\rangle |i_3\rangle \dots |i_n\rangle &= |1_1\rangle (-1)^{i_2} (-1)^{i_3} \dots (-1)^{i_n} |i_2\rangle |i_3\rangle \dots |i_n\rangle, \end{aligned} \quad (15)$$

which shows that when the control qubit 1 is in the state  $|1\rangle$ , a phase flip (from sign  $+$  to  $-$ ) happens to the state  $|1\rangle$  of each of target qubits  $(2, 3, \dots, n)$ , while nothing happens to the states of each of target qubit  $(2, 3, \dots, n)$  when the control qubit 1 is in the state  $|0\rangle$ . From Eq. (8), it can be seen that the jointed unitary operators  $U_1 [\otimes_{l=2}^n U_{1l}]$  involved in Eq. (15) is equivalent to the unitary operator  $U$ . By comparing Eq. (15) with Eq. (1), one can see that a multi-target-qubit controlled phase gate, described by Eq. (1), is realized with  $n$  MP qubits  $(1, 2, \dots, n)$ , after the above operation, described by the unitary operator  $U$ .

We stress that the gate is realized through a single unitary operator  $U$ , which was obtained by starting with the original Hamiltonian (2). In this sense, the gate is implemented with only a single operation. In addition, it is noted that the qutrit remains in the ground state  $|g\rangle$  during the gate operation. Hence, decoherence from the qutrit is greatly suppressed.

In above, we have set  $\chi_{1l} = \chi$ , which turns out into

$$\frac{g_1^2 g_l^2}{4\Delta_{1l}} \left( \frac{1}{\delta_1} + \frac{1}{\delta_l} \right)^2 = \chi. \quad (16)$$



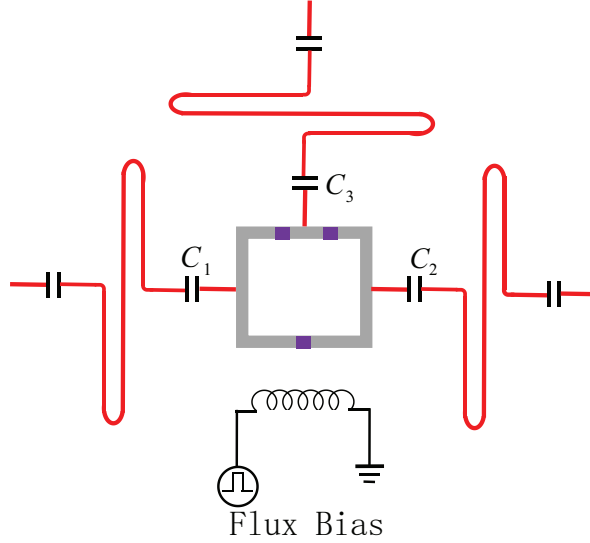


FIG. 3: Setup for three one-dimensional transmission line resonators capacitively coupled to a superconducting flux qutrit.

In addition, we have set  $\chi t = \pi$  and  $\eta t = 2m\pi$ , from which we obtain

$$\frac{g_1^2}{\delta_1} = (2m - n + 1) \chi. \quad (17)$$

Given  $g_1$ ,  $\delta_1$ ,  $m$ , and  $n$ , the value of  $\chi$  can be calculated based on Eq. (17). In addition, given  $g_1$ ,  $\delta_1$ , and  $\chi$ , Eq. (16) can be satisfied by varying  $g_l$  or  $\delta_l$  or both. Note that the detuning  $\delta_l$  can be adjusted by varying the frequency of cavity  $l$ , and the coupling strength  $g_l$  can be adjusted by a prior design of the sample with appropriate capacitance or inductance between the qutrit and cavity  $l$  [13,78].

As shown above, the Hamiltonian (5) was obtained from the Hamiltonian (4) when the levels  $|e\rangle$  and  $|f\rangle$  are initially not occupied. This derivation has nothing to do with  $\Delta_{kl}$ . In this sense, one can have  $\Delta_{kl} \neq 0$  or  $\Delta_{kl} = 0$ . Note that  $\Delta_{kl} = \delta_l - \delta_k = \omega_{c_k} - \omega_{c_l}$ . Thus, the frequencies of cavities (2, 3, ...,  $n$ ) can be chosen to be different or the same. However, it is suggested that for circuit QED, the frequencies of cavities should be different in order to suppress the unwanted inter-cavity crosstalk.

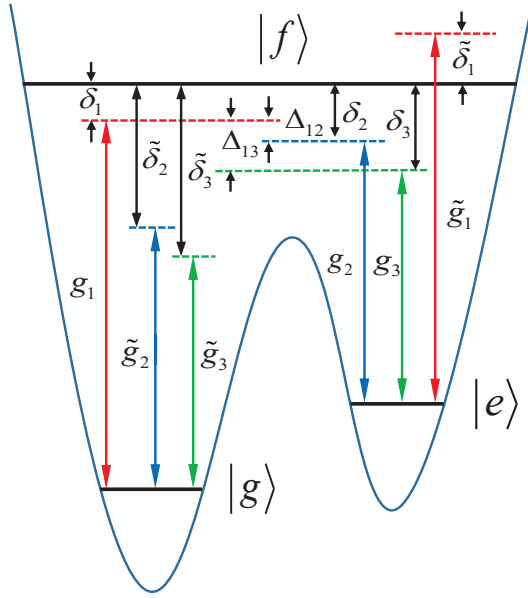


FIG. 4: Illustration of the unwanted coupling between cavity 1 and the  $|e\rangle \leftrightarrow |f\rangle$  transition of the qutrit (with coupling strength  $\tilde{g}_1$  and detuning  $\tilde{\delta}_1$ ) as well as the unwanted coupling between cavity  $l$  and the  $|g\rangle \leftrightarrow |f\rangle$  transition of the qutrit (with coupling strength  $\tilde{g}_l$  and detuning  $\tilde{\delta}_l$ ) ( $l = 2, 3$ ). Note that the coupling of each cavity with the  $|g\rangle \leftrightarrow |e\rangle$  transition of the qutrit is negligible because of the weak  $|g\rangle \leftrightarrow |f\rangle$  transition.

### III. POSSIBLE EXPERIMENTAL IMPLEMENTATION

In this section, we briefly discuss the experimental feasibility of realizing a three-qubit controlled phase gate with one MP qubit simultaneously controlling two target MP qubits, by considering a setup of three microwave cavities (1, 2, 3) coupled to a superconducting flux qutrit (Fig. 3). Each cavity considered in Fig. 3 is a one-dimensional transmission line resonator (TLR).

In reality, there exist the inter-cavity crosstalk between cavities [79], the unwanted coupling of cavity 1 with the  $|e\rangle \leftrightarrow |f\rangle$  transition, and the unwanted coupling of cavities 2 and 3 with the  $|g\rangle \leftrightarrow |f\rangle$  transition of the qutrit (Fig. 4). After taking these factors into account, the Hamiltonian (2) is modified as

$$\tilde{H}_I = H_I + \delta H + \varepsilon, \quad (18)$$

with

$$\begin{aligned} \delta H = & \tilde{g}_1(e^{-i\tilde{\delta}_1 t}\hat{a}_1^+\sigma_{fe}^- + h.c.) \\ & + \sum_{l=2}^3 \tilde{g}_l(e^{-i\tilde{\delta}_l t}\hat{a}_l^+\sigma_{fg}^- + h.c.), \end{aligned} \quad (19)$$

$$\varepsilon = \sum_{k \neq l; k, l=1}^3 g_{kl}(e^{i\tilde{\Delta}_{kl} t}\hat{a}_k^+\hat{a}_l + h.c.). \quad (20)$$

Here,  $H_1$  is the Hamiltonian (2) for  $n = 3$ .  $\delta H$  is the Hamiltonian, which describes the unwanted coupling between cavity 1 and the  $|e\rangle \leftrightarrow |f\rangle$  transition with coupling strength  $\tilde{g}_1$  and detuning  $\tilde{\delta}_1 = \omega_{fe} - \omega_{c_1}$ , as well as the unwanted coupling between cavity  $l$  and the  $|g\rangle \leftrightarrow |f\rangle$  transition with coupling strength  $\tilde{g}_l$  and detuning  $\tilde{\delta}_l = \omega_{fg} - \omega_{c_l}$  ( $l = 2, 3$ ) (Fig. 4). In addition,  $\varepsilon$  represents the inter-cavity crosstalk, with the coupling strength  $g_{kl}$  between cavities  $k$  and  $l$ , as well as the frequency difference  $\tilde{\Delta}_{kl} = \omega_{c_k} - \omega_{c_l}$  of cavities  $k$  and  $l$  ( $k \neq l; k, l \in \{1, 2, 3\}$ ).

When the dissipation and dephasing are included, the dynamics of the lossy system is determined by

$$\begin{aligned} \frac{d\rho}{dt} = & -i[\tilde{H}_1, \rho] + \sum_{l=1}^3 \kappa_l \mathcal{L}[a_l] \\ & + \gamma_{eg} \mathcal{L}[\sigma_{eg}^-] + \gamma_{fe} \mathcal{L}[\sigma_{fe}^-] + \gamma_{fg} \mathcal{L}[\sigma_{fg}^-] \\ & + \sum_{j=e, f} \{\gamma_{\varphi j}(\sigma_{jj} \rho \sigma_{jj} - \sigma_{jj} \rho / 2 - \rho \sigma_{jj} / 2)\}, \end{aligned} \quad (21)$$

where  $\tilde{H}_1$  is the above full Hamiltonian;  $\sigma_{eg}^- = |g\rangle\langle e|$ ,  $\sigma_{jj} = |j\rangle\langle j|$  ( $j = e, f$ ); and  $\mathcal{L}[\xi] = \xi \rho \xi^\dagger - \xi^\dagger \xi \rho / 2 - \rho \xi^\dagger \xi / 2$ , with  $\xi = a_l, \sigma_{eg}^-, \sigma_{fe}^-, \sigma_{fg}^-$ . In addition,  $\kappa_l$  is the photon decay rate of cavity  $l$  ( $l = 1, 2, 3$ ),  $\gamma_{eg}$  is the energy relaxation rate for the level  $|e\rangle$  of the qutrit,  $\gamma_{fe}$  ( $\gamma_{fg}$ ) is the energy relaxation rate of the level  $|f\rangle$  of the qutrit for the decay path  $|f\rangle \rightarrow |e\rangle$  ( $|g\rangle$ ), and  $\gamma_{\varphi j}$  is the dephasing rate of the level  $|j\rangle$  ( $j = e, f$ ) of the qutrit.

The fidelity of the operation is given by

$$\mathcal{F} = \sqrt{\langle \psi_{\text{id}} | \rho | \psi_{\text{id}} \rangle}, \quad (22)$$

where  $|\psi_{\text{id}}\rangle$  is the output state of an ideal system without dissipation, dephasing and crosstalk; while  $\rho$  is the final practical density operator of the system when the operation is performed in a realistic situation. For simplicity, we consider the three qubits are

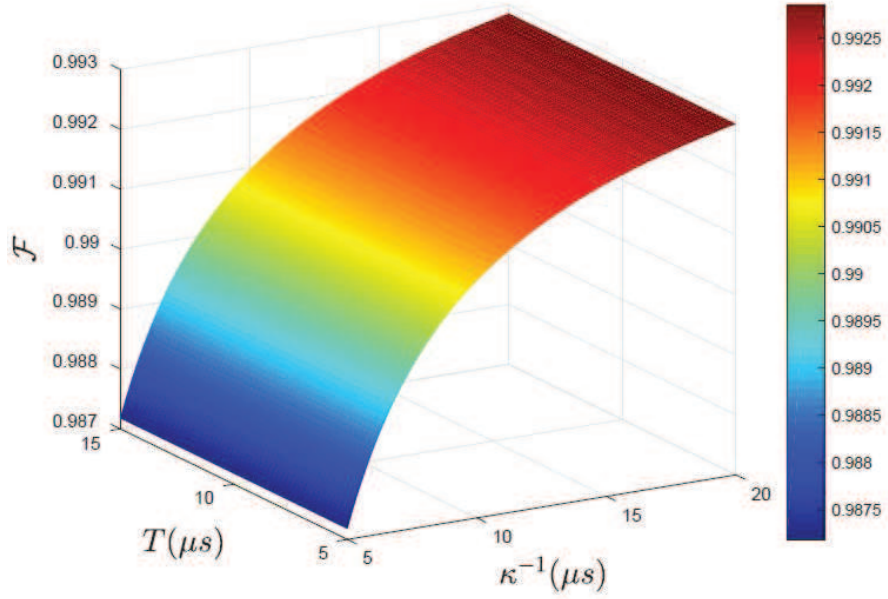


FIG. 5: Fidelity versus  $T$  and  $\kappa^{-1}$ . The parameters used in the numerical simulation are referred to the text.

initially in the following state

$$\begin{aligned}
 |\psi_{\text{in}}\rangle = & \frac{1}{2\sqrt{2}} (|000\rangle + |001\rangle + |010\rangle + |011\rangle \\
 & + |100\rangle + |101\rangle + |110\rangle + |111\rangle). \quad (23)
 \end{aligned}$$

Thus, the ideal output state of the whole system is

$$\begin{aligned}
 |\psi_{\text{id}}\rangle = & \frac{1}{2\sqrt{2}} (|000\rangle + |001\rangle + |010\rangle + |011\rangle \\
 & + |100\rangle - |101\rangle - |110\rangle + |111\rangle) \otimes |g\rangle. \quad (24)
 \end{aligned}$$

For a flux qutrit, the typical transition frequency between neighboring levels can be made as 1 to 20 GHz. As an example, we consider  $\omega_{eg}/2\pi = 5.0$  GHz,  $\omega_{fe}/2\pi = 7.5$  GHz, and  $\omega_{fg}/2\pi = 12.5$  GHz. By choosing  $\delta_1/2\pi = 1.5$  GHz,  $\delta_2/2\pi = 1.51$  GHz, and  $\delta_3/2\pi = 1.53$  GHz, we have  $\Delta_{12}/2\pi = 10$  MHz,  $\Delta_{13}/2\pi = 30$  MHz,  $\omega_{c1}/2\pi = 11$  GHz,  $\omega_{c2}/2\pi = 5.99$  GHz, and  $\omega_{c3}/2\pi = 5.97$  GHz, for which we have  $\tilde{\Delta}_{12}/2\pi = 5.01$  GHz,  $\tilde{\Delta}_{23}/2\pi = 0.02$  GHz, and  $\tilde{\Delta}_{13}/2\pi = 5.03$  GHz. With the transition frequencies of the qutrit and the frequencies of the cavities given here, we have  $\tilde{\delta}_1/2\pi = -3.5$  GHz,  $\tilde{\delta}_2/2\pi = 6.51$  GHz, and  $\tilde{\delta}_3/2\pi = 6.53$  GHz. Other parameters used in the numerical simulation are: (i)  $\gamma_{eg}^{-1} = 5T$   $\mu\text{s}$ ,  $\gamma_{fe}^{-1} = 2T$

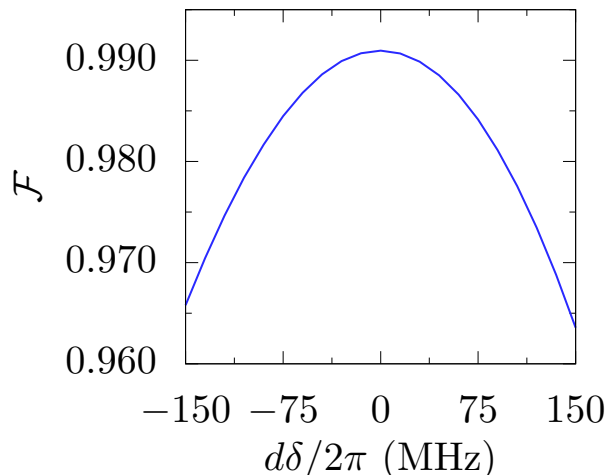


FIG. 6: Fidelity versus  $d\delta$ . Here,  $d\delta$  is the detuning error, which applies to each of detunings  $\delta_1, \delta_2$ , and  $\delta_3$ . The figure is plotted for  $T = 5 \mu\text{s}$  and  $\kappa^{-1} = 10 \mu\text{s}$ . Other parameters used in the numerical simulation are the same as those used in Fig. 5.

$\mu\text{s}$ ,  $\gamma_{fg}^{-1} = T \mu\text{s}$ , (ii)  $\gamma_{\phi e}^{-1} = \gamma_{\phi f}^{-1} = T \mu\text{s}$ , and (iii)  $g_1/2\pi = 150 \text{ MHz}$ . According to Eqs. (16) and (17), one can calculate the  $g_2$  and  $g_3$ , which are  $g_2/2\pi \sim 86.89 \text{ MHz}$  and  $g_3/2\pi \sim 151.49 \text{ MHz}$ . For a flux qutrit, one has  $\tilde{g}_1 \sim g_1$ ,  $\tilde{g}_2 \sim g_2$ , and  $\tilde{g}_3 \sim g_3$ . Note that the coupling constants chosen here are readily available because a coupling constant  $\sim 2\pi \times 636 \text{ MHz}$  has been reported for a flux device coupled to a one-dimensional transmission line resonator [40]. We set  $g_{kl} = 0.01g_{\text{max}}$ , where  $g_{\text{max}} = \max\{g_1, g_2, g_3\} \sim 2\pi \times 151.49 \text{ MHz}$ , which can be achieved in experiments [56,69]. In addition, assume  $\kappa_1 = \kappa_2 = \kappa_3 = \kappa$  for simplicity.

By solving the master equation (21), we numerically calculate the fidelity versus  $T$  and  $\kappa^{-1}$ , as depicted in Fig. 5. From Fig. 5, one can see that when  $T \geq 5 \mu\text{s}$  and  $\kappa^{-1} \geq 10 \mu\text{s}$ , fidelity exceeds 0.9909, which implies that a high fidelity can be obtained for the gate being performed in a realistic situation.

To investigate the effect of the detuning errors on the fidelity, we consider a small deviation  $d\delta$  for  $\delta_1, \delta_2$ , and  $\delta_3$ . Thus, we modify  $\delta_1, \delta_2$ , and  $\delta_3$  as  $\delta_1 + d\delta, \delta_2 + d\delta$ , and  $\delta_3 + d\delta$ . With this modification, we numerically calculate the fidelity for  $T = 5 \mu\text{s}$  and  $\kappa^{-1} = 10 \mu\text{s}$  and plot Fig. 6 showing the fidelity versus  $d\delta$ . From Fig. 6, one can see that the fidelity can reach 0.98 or greater for  $-75 \text{ MHz} \leq d\delta/2\pi \leq 75 \text{ MHz}$ .

The gate operational time is estimated as  $\sim 66.7 \text{ ns}$  for the parameters chosen above,

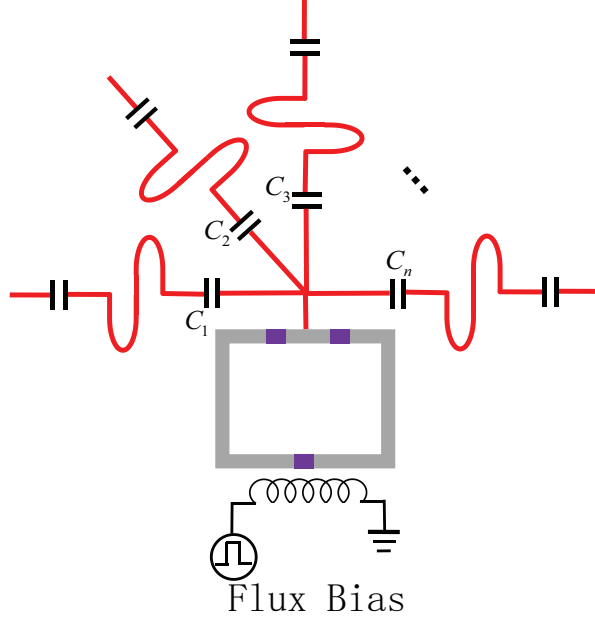


FIG. 7: Schematic diagram for  $n$  cavities coupled by a superconducting flux qutrit. Each cavity here is a one-dimensional transmission line resonator, which is coupled to the qutrit via a capacitor.

which is much shorter than the decoherence times of the qutrit ( $5 \mu\text{s} - 75 \mu\text{s}$ ) and the cavity decay times ( $5 \mu\text{s} - 20 \mu\text{s}$ ) considered in Fig. 5. Here, we consider a rather conservative case for decoherence time of the flux qutrit because decoherence time  $70 \mu\text{s}$  to  $1 \text{ms}$  has been experimentally reported for a superconducting flux device [32,36,38]. For the cavity frequencies given above and  $\kappa^{-1} = 10 \mu\text{s}$ , one has  $Q_1 \sim 6.9 \times 10^5$  for cavity 1,  $Q_2 \sim 3.76 \times 10^5$  for cavity 2, and  $Q_3 \sim 3.75 \times 10^5$  for cavity 3, which are available because TLRs with a (loaded) quality factor  $Q \sim 10^6$  have been experimentally demonstrated [42,43]. The analysis here implies that high-fidelity realization of a quantum controlled phase gate with one MP qubit simultaneously controlling two target MP qubits is feasible with the present circuit QED technology.

In above, we have provided the specific implementation of the three qubits case. For the gate with more than three qubits, the extension is straightforward. From Fig. 7, one can see that each of the multiple cavities can in principle be coupled to a single superconducting flux qutrit via a capacitor. However, it should be pointed out that in the solid-state setup scaling up to many cavities coupled to one qutrit will introduce new challenges. For instance, the cavity crosstalk may become worse as the number of cavities increases, which will decrease

the operation fidelity.

#### IV. CONCLUSION

We have presented a one-step approach to realize an  $n$ -qubit controlled phase gate with one microwave photonic qubit simultaneously controlling  $n - 1$  target microwave photonic qubits, based on circuit QED. As shown above, this proposal has the following advantages: (i) During the gate operation, the qutrit remains in the ground state; thus decoherence from the qutrit is greatly suppressed; (ii) Because only one-step operation is needed and neither classical pulse nor measurement is required, the gate implementation is simple; (iii) The gate operation time is independent of the number of the qubits; and (iv) This proposal is quite general and can be applied to realize the proposed gate with a wide range of physical systems, such as multiple microwave or optical cavities coupled to a single  $\Lambda$ -type three-level natural or artificial atom. Furthermore, our numerical simulations demonstrate that high-fidelity implementation of a three-qubit controlled phase gate with one microwave photonic qubit simultaneously controlling two target microwave photonic qubits is feasible with present circuit QED technology. We hope that this work will stimulate experimental activities in the near future.

#### Acknowledgment

This work was supported in part by the NKRD of China (Grant No. 2016YFA0301802) and the National Natural Science Foundation of China under Grant Nos. [11074062, 11374083, 11774076]. This work was also supported by the Hangzhou-City grant for Quantum Information and Quantum Optics Innovation Research Team.

- 
- [1] L. M. Duan, B. Wang, and H. J. Kimble, “Robust quantum gates on neutral atoms with cavity-assisted photon-scattering”, *Phys. Rev. A* **72**, 032333 (2005).
  - [2] X. Wang, A. Sørensen, and K. Mølmeret, “Multibit Gates for Quantum Computing”, *Phys. Rev. Lett.* **86**, 3907 (2001).

- [3] C. P. Yang and S. Han, “n-qubit-controlled phase gate with superconducting quantum-interference devices coupled to a resonator”, *Phys. Rev. A* **72**, 032311 (2005).
- [4] X. Zou, Y. Dong, and G. C. Guo, “Implementing a conditional z gate by a combination of resonant interaction and quantum interference”, *Phys. Rev. A* **74**, 032325 (2006).
- [5] C. P. Yang and S. Han, “Realization of an n-qubit controlled-U gate with superconducting quantum interference devices or atoms in cavity QED”, *Phys. Rev. A* **73**, 032317 (2006).
- [6] T. Monz, K. Kim, W. Hänsel, M. Riebe, A. S.Villar, P. Schindler, M. Chwalla, M. Hennrich, and R. Blatt, “Realization of the Quantum Toffoli Gate with Trapped Ions”, *Phys. Rev. Lett.* **102**, 040501 (2009).
- [7] W. L. Yang, Z. Q. Yin, Z. Y. Xu, M. Feng, and J. F. Du, “One step implementation of multi-qubit conditional phase gating with nitrogen-vacancy centers coupled to a high-Q silicamicro sphere cavity”, *Appl. Phys. Lett.* **96**, 241113 (2010).
- [8] S. B. Zheng, “Implementation of Toffoli gates with a single asymmetric Heisenberg XY interaction”, *Phys. Rev. A* **87**, 042318 (2013).
- [9] H. R. Wei and F. G. Deng, “Universal quantum gates for hybrid systems assisted by quantum dots inside double-sided optical microcavities”, *Phys. Rev. A* **87**, 022305 (2013).
- [10] H. W. Wei and F. G. Deng, “Scalable quantum computing based on stationary spin qubits in coupled quantum dots inside double-sided optical microcavities”, *Sci. Rep.* **4**, 7551 (2014).
- [11] M. Hua, M. J. Tao, and F. G. Deng, “Universal quantum gates on microwave photons assisted by circuit quantum electrodynamics”, *Phys. Rev. A* **90**, 012328 (2014).
- [12] M. Hua, M. J. Tao, and F. G. Deng, “Fast universal quantum gates on microwave photons with all-resonance operations in circuit QED”, *Sci. Rep.* **5**, 9274 (2015).
- [13] B. Ye, Z. F. Zheng, and C. P. Yang, “Multiplex-controlled phase gate with qubits distributed in a multicavity system”, *Phys. Rev. A* **97**, 062336 (2018).
- [14] Q. Wei, X. Wang, A. Miranowicz, Z. Zhong, and F. Nori, “Heralded quantum controlled-PHASE gates with dissipative dynamics in macroscopically distant resonators”, *Phys. Rev. A* **96**, 012315 (2017).
- [15] M. Šašura and V. Buzek, “Multiparticle entanglement with quantum logic networks: Application to cold trapped ions”, *Phys. Rev. A* **64**, 012305 (2001).
- [16] F. Gaitan, *Quantum Error Correction and Fault Tolerant Quantum Computing* (CRC Press, USA, 2008).



- [17] T. Beth and M. Rötteler, *Quantum Information* (Springer, Berlin, 2001), Vol. 173, Ch. 4, p. 96.
- [18] S. L. Braunstein, V. Bužek, and M. Hillery, “Quantum network for symmetric and asymmetric cloning in arbitrary dimension and continuous limit”, *Phys. Rev. A* **63**, 052313 (2001).
- [19] C. P. Yang, Y. X. Liu, and F. Nori, “Phase gate of one qubit simultaneously controlling  $n$  qubits in a cavity”, *Phys. Rev. A* **81**, 062323 (2010).
- [20] C. P. Yang, S. B. Zheng, and F. Nori, “Multiqubit tunable phase gate of one qubit simultaneously controlling  $n$  qubits in a cavity”, *Phys. Rev. A* **82**, 062326 (2010).
- [21] H. F. Wang, A. D. Zhu, and S. Zhang, “One-step implementation of multiqubit phase gate with one control qubit and multiple target qubits in coupled cavities”, *Opt. Lett.* **39**, 1489-1492 (2014).
- [22] C. P. Yang, Q. P. Su, F. Y. Zhang, and S. B. Zheng, “Single-step implementation of a multiple-target-qubit controlled phase gate without need of classical pulses”, *Opt. Lett.* **39**, 3312-3315 (2014).
- [23] T. Liu, X. Z. Cao, Q. P. Su, S. J. Xiong, and C. P. Yang, “Multi-target-qubit unconventional geometric phase gate in a multicavity system”, *Sci. Rep.* **6**, 21562 (2016).
- [24] J. Clarke and F. K. Wilhelm, “Superconducting quantum bits”, *Nature* **453**, 1031-1042 (2008).
- [25] I. Buluta, S. Ashhab, and F. Nori, “Natural and artificial atoms for quantum computation”, *Rep. Prog. Phys.* **74**, 104401-104416 (2011).
- [26] J. Q. You and F. Nori, “Atomic physics and quantum optics using superconducting circuits”, *Nature (London)* **474**, 589-597 (2011).
- [27] Z. L. Xiang, S. Ashhab, J. Q. You, and F. Nori, “Hybrid quantum circuits: Superconducting circuits interacting with other quantum systems”, *Rev. Mod. Phys.* **85**, 623-653 (2013).
- [28] J. Q. You and F. Nori, “Superconducting circuits and quantum information”, *Phys. Today* **58**, 42-47 (2005).
- [29] X. Gu, A. F. Kockum, A. Miranowicz, Y. X. Liu, and F. Nori, “Microwave photonics with superconducting quantum circuits”, *Phys. Rep.* **718**, 1-102 (2017).
- [30] J. Bylander, S. Gustavsson, F. Yan, F. Yoshihara, K. Harrabi, G. F. David, G. Cory, Y. Nakamura, J. S. Tsai, and W. D. Oliver, “Noise spectroscopy through dynamical decoupling with a superconducting flux qubit”, *Nat. Phys.* **7**, 565-570 (2011).
- [31] H. Paik, D. I. Schuster, L. S. Bishop, G. Kirchmair, G. Catelani, A. P. Sears, B. R. Johnson,

- M. J. Reagor, L. Frunzio, L. I. Glazman, S. M. Girvin, M. H. Devoret, and R. J. Schoelkopf, “Observation of high coherence in josephson junction qubits measured in a three-dimensional circuit QED architecture”, *Phys. Rev. Lett.* **107**, 240501 (2011).
- [32] C. Rigetti, S. Poletto, J. M. Gambetta, B. L. T. Plourde, J. M. Chow, A. D. Corcoles, J. A. Smolin, S. T. Merkel, J. R. Rozen, G. A. Keefe, M. B. Rothwell, M. B. Ketchen, and M. Steffen, “Superconducting qubit in waveguide cavity with coherence time approaching 0.1 ms”, *Phys. Rev. B* **86**, 100506(R) (2012).
- [33] R. Barends, J. Kelly, A. Megrant, D. Sank, E. Jeffrey, Y. Chen, Y. Yin, B. Chiaro, J. Mutus, C. Neill, P. O’Malley, P. Roushan, J. Wenner, T. C. White, A. N. Cleland, and J. M. Martinis, “Coherent Josephson qubit suitable for scalable quantum integrated circuits”, *Phys. Rev. Lett.* **111**, 080502 (2013).
- [34] Y. Chen, C. Neill, P. Roushan, N. Leung, M. Fang, R. Barends, J. Kelly, B. Campbell, Z. Chen, B. Chiaro, A. Dunsworth, E. Jeffrey, A. Megrant, J. Y. Mutus, P. J. J. O’Malley, C. M. Quintana, D. Sank, A. Vainsencher, J. Wenner, T. C. White, Michael R. Geller, A. N. Cleland, and J. M. Martinis, “Qubit architecture with high coherence and fast tunable coupling”, *Phys. Rev. Lett.* **113**, 220502 (2014).
- [35] M. Stern, G. Catelani, Y. Kubo, C. Grezes, A. Bienfait, D. Vion, D. Esteve, and P. Bertet, “Flux qubits with long coherence times for hybrid quantum circuits”, *Phys. Rev. Lett.* **113**, 123601 (2014).
- [36] I. M. Pop, K. Geerlings, G. Catelani, R. J. Schoelkopf, L. I. Glazman, and M. H. Devoret, “Coherent suppression of electromagnetic dissipation due to superconducting quasiparticles”, *Nature (London)* **508**, 369-372 (2014).
- [37] M. J. Peterer, S. J. Bader, X. Jin, F. Yan, A. Kamal, T. J. Gudmundsen, P. J. Leek, T. P. Orlando, W. D. Oliver, and S. Gustavsson, “Coherence and decay of higher energy levels of a superconducting transmon qubit”, *Phys. Rev. Lett.* **114**, 010501 (2015).
- [38] F. Yan, S. Gustavsson, A. Kamal, J. Birenbaum, A. P. Sears, D. Hover, T. J. Gudmundsen, J. L. Yoder, T. P. Orlando, J. Clarke, A. J. Kerman, and W. D. Oliver, “The Flux Qubit Revisited to Enhance Coherence and Reproducibility”, *Nat. Commun.* **7**, 12964 (2016); J. Q. You, X. Hu, S. Ashhab, and F. Nori, “Low-decoherence flux qubit”, *Phys. Rev. B* **75**, 140515(R) (2007).
- [39] A. Wallraff, D. I. Schuster, A. Blais, L. Frunzio, R. S. Huang, J. Majer, S. Kumar, S. M.

- Girvin, and R. J. Schoelkopf, “Strong coupling of a single photon to a superconducting qubit using circuit quantum electrodynamics”, *Nature (London)* **431**, 162-167 (2004).
- [40] T. Niemczyk, F. Deppe, H. Huebl, E. P. Menzel, F. Hocke, M. J. Schwarz, J. J. Garcia Ripoll, D. Zueco, T. Hümmer, E. Solano, A. Marx, and R. Gross, “Circuit quantum electrodynamics in the ultrastrong-coupling regime”, *Nat. Phys.* **6**, 772-776 (2010).
- [41] A. F. Kockum, A. Miranowicz, S. D. Liberato, S. Savasta, and F. Nori, “Ultrastrong coupling between light and matter”, arXiv:1807.11636.
- [42] W. Chen, D. A. Bennett, V. Patel, and J. E. Lukens, “Substrate and process dependent losses in superconducting thin film resonators”, *Supercond. Sci. Technol.* **21**, 075013 (2008).
- [43] P. J. Leek, M. Baur, J. M. Fink, R. Bianchetti, L. Steffen, S. Filipp, and A. Wallraff, “Cavity quantum electrodynamics with separate photon storage and qubit readout modes”, *Phys. Rev. Lett.* **104**, 100504 (2010).
- [44] M. Reagor, W. Pfaff, C. Axline, R. W. Heeres, N. Ofek, K. Sliwa, E. Holland, C. Wang, J. Blumoff, K. Chou, M. J. Hatridge, L. Frunzio, M. H. Devoret, L. Jiang, and R. J. Schoelkopf, “A quantum memory with near-millisecond coherence in circuit QED”, *Phys. Rev. B* **94**, 014506 (2016).
- [45] C. P. Yang, S. I. Chu, and S. Han, “Possible realization of entanglement, logical gates, and quantum-information transfer with superconducting-quantum-interference-device qubits in cavity QED”, *Phys. Rev. A* **67**, 042311 (2003).
- [46] J. Q. You and F. Nori, “Quantum information processing with superconducting qubits in a microwave field”, *Phys. Rev. B* **68**, 064509 (2003).
- [47] A. Blais, R. S. Huang, A. Wallraff, S. M. Girvin, and R. J. Schoelkopf, “Cavity quantum electrodynamics for superconducting electrical circuits: An architecture for quantum computation”, *Phys. Rev. A* **69**, 062320 (2004).
- [48] M. Hofheinz, H. Wang, M. Ansmann, R. C. Bialczak, E. Lucero, M. Neeley, A. D. O’Connell, D. Sank, J. Wenner, J. M. Martinis, and A. N. Cleland, “Synthesizing arbitrary quantum states in a superconducting resonator”, *Nature (London)* **459**, 546-549 (2009).
- [49] H. Wang, M. Hofheinz, J. Wenner, M. Ansmann, R. C. Bialczak, M. Lenander, E. Lucero, M. Neeley, A. D. O’Connell, D. Sank, M. Weides, A. N. Cleland, and J. M. Martinis, “Improving the Coherence Time of Superconducting Coplanar Resonators”, *Appl. Phys. Lett.* **95**, 233508 (2009).

- [50] M. H. Devoret and R. J. Schoelkopf, “Superconducting circuits for quantum information: an outlook”, *Science* **339**, 1169-1174 (2013).
- [51] Y. X. Liu, L. F. Wei, and F. Nori, “Generation of nonclassical photon states using a superconducting qubit in a microcavity”, *Europhys. Lett.* **67**, 941-947 (2004).
- [52] M. Hofheinz, E. M. Weig, M. Ansmann, R. C. Bialczak, E. Lucero, M. Neeley, A. D. O’Connell, H. Wang, J. M. Martinis, and A. N. Cleland, “Generation of fock states in a superconducting quantum circuit”, *Nature (London)* **454**, 310-314 (2008).
- [53] F. W. Strauch, K. Jacobs, and R. W. Simmonds, “Arbitrary control of entanglement between two superconducting resonators”, *Phys. Rev. Lett.* **105**, 050501 (2010).
- [54] Q. P. Su, C. P. Yang, and S. B. Zheng, “Fast and simple scheme for generating NOON states of photons in circuit QED”, *Sci. Rep.* **4**, 3898 (2014).
- [55] M. Hua, M. J. Tao, and F. G. Deng, “Universal quantum gates on microwave photons assisted by circuit quantum electrodynamics”, *Phys. Rev. A* **90**, 18824 (2014).
- [56] S. J. Xiong, Z. Sun, J. M. Liu, T. Liu, and C. P. Yang, “Efficient scheme for generation of photonic NOON states in circuit QED”, *Opt. Lett.* **40**, 2221-2224 (2015).
- [57] M. Hua, M. J. Tao, and F. G. Deng, “Quantum state transfer and controlled-phase gate on one-dimensional superconducting resonators assisted by a quantum bus”, *Sci. Rep.* **6**, 22037 (2016).
- [58] A. N. Korotkov, “Flying microwave qubits with nearly perfect transfer efficiency”, *Phys. Rev. B* **84**, 014510 (2011).
- [59] E. A. Sete, E. Mlinar, and A. N. Korotkov, “Robust quantum state transfer using tunable couplers”, *Phys. Rev. B* **91**, 144509 (2015).
- [60] H. Wang, M. Mariani, R. C. Bialczak, M. Lenander, E. Lucero, M. Neeley, A. D. O’Connell, D. Sank, M. Weides, J. Wenner, T. Yamamoto, Y. Yin, J. Zhao, J. M. Martinis, and A. N. Cleland, “Deterministic entanglement of photons in two superconducting microwave resonators”, *Phys. Rev. Lett.* **106**, 060401 (2011).
- [61] S. J. Srinivasan, N. M. Sundaresan, D. Sadri, Y. Liu, J. M. Gambetta, T. Yu, S. M. Girvin, and A. A. Houck, “Time-reversal symmetrization of spontaneous emission for quantum state transfer”, *Phys. Rev. A* **89**, 033857 (2014).
- [62] J. Wenner, Y. Yin, Y. Chen, R. Barends, B. Chiaro, E. Jeffrey, J. Kelly, A. Megrant, J. Y. Mutus, C. Neill, P. J. J. O’Malley, P. Roushan, D. Sank, A. Vainsencher, T. C. White, A. N.

- Korotkov, A. N. Cleland, and J. M. Martinis, “Catching Time-Reversed Microwave Coherent State Photons with 99.4% Absorption Efficiency”, *Phys. Rev. Lett.* **112**, 210501 (2014).
- [63] C. P. Yang, Q. P. Su, and S. Y. Han, “Generation of Greenberger-Horne-Zeilinger entangled states of photons in multiple cavities via a superconducting qutrit or an atom through resonant interaction”, *Phys. Rev. A* **86**, 022329 (2012).
- [64] C. P. Yang, Q. P. Su, S. B. Zheng, and S. Han, “Generating entanglement between microwave photons and qubits in multiple cavities coupled by a superconducting qutrit”, *Phys. Rev. A* **87**, 022320 (2013).
- [65] S. E. Nigg, “Deterministic hadamard gate for microwave cat-state qubits in circuit QED”, *Phys. Rev. A* **89**, 022340 (2014).
- [66] R. W. Heeres, P. Reinhold, N. Ofek, L. Frunzio, L. Jiang, M. H. Devoret, and R. J. Schoelkopf, “Implementing a universal gate set on a logical qubit encoded in an oscillator”, *arXiv:1608.02430* (2016).
- [67] C. P. Yang, Q. P. Su, S. B. Zheng, F. Nori, and S. Han, “Entangling two oscillators with arbitrary asymmetric initial states”, *Phys. Rev. A* **95**, 052341 (2017).
- [68] C. Wang, Y. Y. Gao, P. Reinhold, R. W. Heeres, N. Ofek, K. Chou, C. Axline, M. Reagor, J. Blumoff, K. M. Sliwa, L. Frunzio, S. M. Girvin, L. Jiang, M. Mirrahimi, M. H. Devoret, and R. J. Schoelkopf, “A Schrodinger Cat Living in Two Boxes”, *Science* **352**, 1087-1091 (2016).
- [69] Y. Zhang, X. Zhao, Z. F. Zheng, L. Yu, Q. P. Su, and C. P. Yang, “Universal controlled-phase gate with cat-state qubits in circuit QED”, *Phys. Rev. A* **96**, 052317 (2017).
- [70] H. F. Wang, A. D. Zhu, S. Zhang, and K. H. Yeon, “Deterministic CNOT gate and entanglement swapping for photonic qubits using a quantum-dot spin in a double-sided optical microcavity”, *Phys. Lett. A* **377**, 2870 (2013).
- [71] C. H. Bai, D. Y. Wang, S. Hu, W. X. Cui, X. X. Jiang, and H. F. Wang, “Scheme for implementing multitarget qubit controlled-NOT gate of photons and controlled-phase gate of electron spins via quantum dot-microcavity coupled system”, *Quantum. Inf. Process* **15**, 1485-1498 (2016).
- [72] J. R. Johansson, N. Lambert, I. Mahboob, H. Yamaguchi, and F. Nori, “Entangled-state generation and Bell inequality violations in nanomechanical resonators”, *Phys. Rev. B* **90**, 174307 (2014).
- [73] P. J. Leek, S. Filipp, P. Maurer, M. Baur, R. Bianchetti, J. M. Fink, M. Göppl, L. Steffen, and

- A. Wallraff, “Using sideband transitions for two-qubit operations in superconducting circuits”, *Phys. Rev. B* **79**, 180511 (2009).
- [74] M. Neeley, M. Ansmann, R. C. Bialczak, M. Hofheinz, N. Katz, E. Lucero, A. O’Connell, H. Wang, A. N. Cleland, and J. M. Martinis, “Process tomography of quantum memory in a Josephson-phase qubit coupled to a two-level state”, *Nat. Phys.* **4**, 523-526 (2008).
- [75] M. Sandberg, C. M. Wilson, F. Persson, T. Bauch, G. Johansson, V. Shumeiko, T. Duty, and P. Delsing, “Tuning the field in a microwave resonator faster than the photon life time”, *Appl. Phys. Lett.* **92**, 203501 (2008).
- [76] Z. L. Wang, Y. P. Zhong, L. J. He, H. Wang, J. M. Martinis, A. N. Cleland, and Q. W. Xie, “Quantum state characterization of a fast tunable superconducting resonator”, *Appl. Phys. Lett.* **102**, 163503 (2013).
- [77] D. F. James and J. Jerke, “Effective Hamiltonian theory and its applications in quantum information”, *Can. J. Phys.* **85**, 625-632 (2007).
- [78] Qi-Ping Su, H. H. Zhu, L. Yu, Y. Zhang, S. J. Xiong, J. M. Liu, and C. P. Yang, “Generating double NOON states of photons in circuit QED”, *Phys. Rev. A* **95**, 022339 (2017).
- [79] C. P. Yang, Q. P. Su, S. B. Zheng, and F. Nori, “Crosstalk-insensitive method for simultaneously coupling multiple pairs of resonators”, *Phys. Rev. A* **93**, 042307 (2016).